CrystEngComm

Accepted Manuscript

ROYAL SOCIETY OF CHEMISTRY

www.rsc.org/crystengcomm

Co-crystals formation between 2-amino-4,6-dimethylpyrimidine and new p-xylylene-bis(thioacetic) acid

A. Ostasz[a], R. Łyszczek[a], L. Mazur[a], B. Tarasiuk[b]

[a]*Department of General and Coordination Chemistry,* [b]*Department of Organic Chemistry, Faculty of Chemistry, Maria Curie-Skłodowska University, M.C. Skłodowska Sq. 2, 20-031 Lublin, Poland;*
email: a.ostasz@poczta.umcs.lublin.pl

Abstract

Novel p-xylylene-bis(thioacetic) acid (*p*-XBTA) and its co-crystals with 2-amino-4,6-dimethyl pyrimidine (DMP) have been synthesized and characterized by the single crystal X-ray diffraction, infrared spectroscopy and thermal analysis methods (TG/DSC). Depending on the crystallization conditions, three different multicomponent crystal forms have been isolated with various chemical compositions and stoichiometries of the co-formers. The ATR-FTIR spectra of co-crystals display the stretching vibrations bands for the co-formers with associated shifts confirming the formation of a new phases. DSC and TG were used to reveal the relative stabilities of new solids compared to those the co-formers.

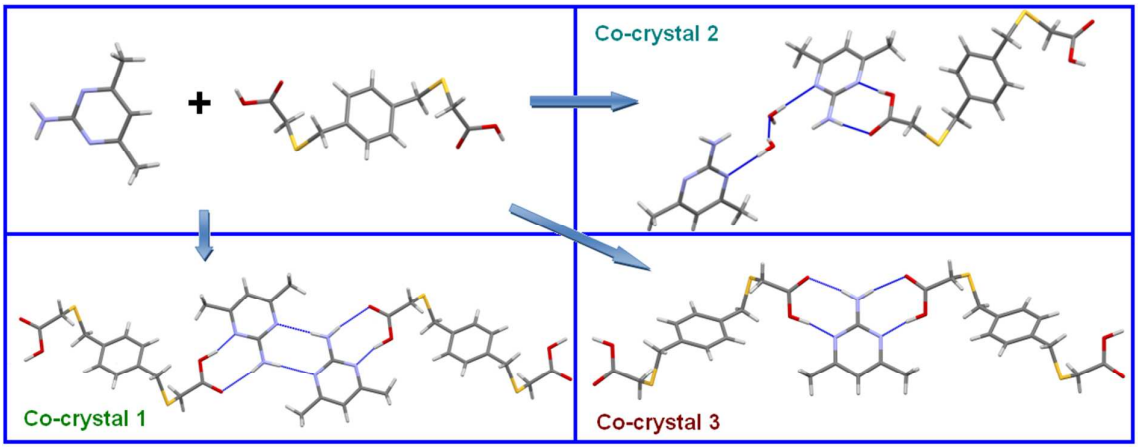

Introduction

Preparation of new compounds with tailor-made properties can be exploited for many purposes such as host-guest compounds,[1, 2] nonlinear optical materials,[3, 4] organic conductors[5] or coordination polymers.[6, 7].

Co-crystals represent a class of compounds that could be reasonably described as long known but little studied. Less than 1% of structurally characterized molecular organics are co-crystals.[8] In 2012 year, 46 authors of article in *Crystal Growth@Design* proposed the

definition of co-crystals consistent with the scientific literature: *co-crystals are solids that are crystalline single phase materials composed of two or more different molecular and/or ionic compounds generally in a stoichiometric ratio which are neither solvates nor simple salts.*[9] Co-crystals offer huge opportunities for the pharmaceutical industry. Co-crystallization can improve final product properties such as solubility, melting point, crystallinity, hydroscopicity and stability.[10]

Pyrimidines and aminopyrimidine derivatives are biologically important compounds that manifest themselves in nature as components of nucleic acids. The functions of nucleic acids are explicitly determined by hydrogen-bonding patterns including base pairing, which is responsible for genetic information transfer. Their interactions with carboxylic acids are involved in protein-nucleic acid recognition and drug-protein recognition processes. Co-crystals of aminopyrimidine with carboxylic acids represent model systems where the hydrogen bonded supramolecular motifs can be studied in detail.[11] Some co-crystal structures of pyrimidine and aminopyrimidine derivatives have been reported earlier.[12] The primary motif in their crystals is the pyrimidine-carboxylic acid dimer through the predominant $R_2^2(8)$[13] synthon, involving the O-H···N and N-H···O hydrogen bonds. Subsequent levels of aggregation form either a linear (LHT) or cyclic heterotetramer (CHT) or heterotrimer (HT) or other preferred stable synthons.[10,11] There are is 33 carboxylic acid: DMP molecular complexes (22 co-crystals and 11 salts) which have been described in the literature so far.[14] The dominant synthon observed in their structures is a LHT one (67% of existing structures). It is worth noting that **co-2** is probably the first example of hydrated form of carboxylic acid: DMP co-crystal, reported so far, as confirmed by the CSD[14] data search.

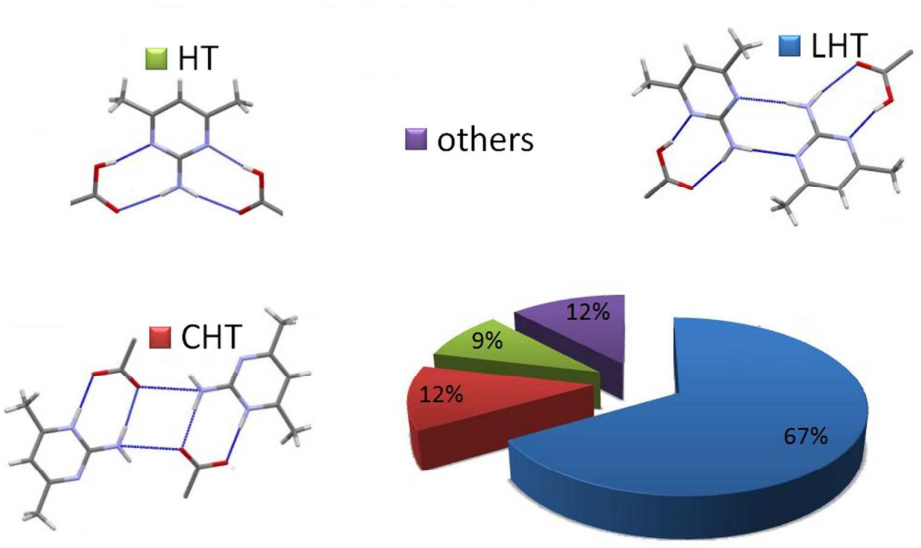

Fig. 1 Presentation of the percentage distribution of types of synthons in the existing structures of DMP and carboxylic acids (LHT- linear heterotetramer, CHT- cyclic heterotetramer, HT- heterotrimer)[14]

In this paper the synthesis, structural and some physicochemical properties of p-xylylenebis-(thioacetic) acid (*p*-XBTA) are presented. The crystal structure of *p*-XBTA has not been reported in literature so far. The acid is derived from a xylylene molecule and contains two carboxylic groups as well as flexible thioaliphatic spacers. As such, this is a potential ligand for construction of coordination polymers. The aim of this study was to explore the capacity of (*p*-XBTA) (Scheme 1b) to form supramolecular assemblies with 2-amino-4,6-dimethyl-pyrimidine (DMP) (Scheme 1a) base as well as to check the influence of synthesis conditions on structure and composition of the resulting co-crystals.

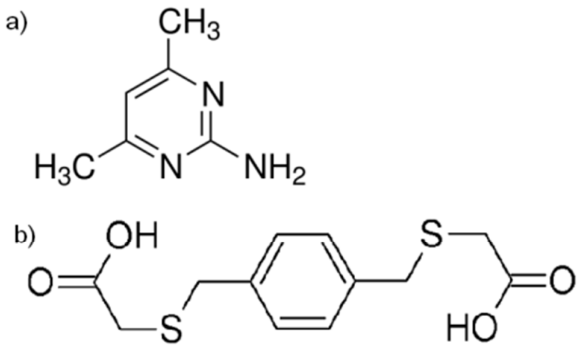

Scheme 1. Molecular structures of **a)** 2-amino-4,6-dimethylpyrimidine (DMP) and **b)** p-xylylenebis-(thioacetic) acid (*p*-XBTA)

Experimental

Synthesis

The co-crystal former, *p*-xylylenebis(thioacetic) acid, was synthesized in four stages (Scheme 2). In the first stage *p*-bis(bromomethyl)benzene (mp[15] 145 °C) was obtained by the action of bromine on *p*-xylene. The resulting compound was heated in ethanol with thiourea. The salt of *p*-diisothiouronium was subjected to basic hydrolysis and then the resulting *p*-phenylene-bis(methanethiol) was condensed with chloroacetic acid in the alkaline medium.

p-Bis(bromomethyl)benzene

p-Xylene (10.6 g, 0.10 mol) was dissolved in tetrachloromethane (100 ml) and 0.5 g of dibenzoyl peroxide was added. The mixture was heated under reflux and bromine (35.5 g, 0.22 mol) was added to a solution of tetrachloromethane dropwise within 20 min. The reaction mixtures were stirred for 5 h and irradiated with UV-lamp. The solvent evaporated under reduced pressure, and the reaction mixtures were crystallized three times from methanol and cyclohexane (70:30, v/v). The residue (13.7 g, 52%) was sufficiently pure. mp 145.5 ^{o}C (ref. [15] mp 145 °C)

Anal. Calc. for $C_8H_8Br_2$ (263.96): C 36.40; H 3.05. Found: C 36.43; H 3.08, ^{1}H NMR ($CDCl_3$): 4.65 (4H, s, -$C_6H_4C\underline{H}2Br$), 7.39-8.11 (4H, m, C_6H_4-$\underline{H}$).

p-Benzene-bis(methanethiol)

Thiourea (9.5 g, 0.125 mol) was added to a solution of α,α′-dibromo-*p*-xylene (13.2 g, 0.05 mol) in acetone (200 ml). The mixture was heated to reflux for 1 h, and then cooled to room temperature. A precipitate of bis(thiouronium) salt was filtered off, and dried under high vacuum. The solid was dissolved in 3M NaOH (100 ml), the mixture was heated to reflux for 3 h, and the solution was neutralized to pH ~2 with hydrochloric acid. Dithiol was extracted into methylene chloride, the organic solution was washed with water, dried over anhydrous Na_2SO_4, and evaporated. The residue (7.4 g, 87%) was sufficiently pure. mp 46 ^oC (ref. [16] mp 46-47 ^oC).

Anal. Calc. for $C_8H_{10}S_2$ (170.30): C 56.42; H 5.92. Found: C 56.43; H 5.89, ^1H NMR ($CDCl_3$): 1.72 (2H, s, -S<u>H</u>), 4.15 (4H, s, -C_6H_4C<u>H_2</u>S), 7.38-8.15 (4H, m, -C_6H_4-<u>H</u>,).

p-Xylylenebis(thioacetic) acid

To the mixture of 8.0 g of sodium hydroxide dissolved in 150 ml of ethanol and 100 ml of water, 8.5 g of 1,4-benzene-bis(methanethiol) (0.05 mol) was added. To this mixture stirred at room temperature, a solution of 9.5 g (0.1 mol) of chloroacetic acid in 50 ml of water was added and the reaction mixture was refluxed for 4 hours, cooled to 0 ^oC and acidified to pH 1 with hydrochloric acid. Crystallization of the crude product from ethanol gave 11.7 g (82 % yield) of pure compound *p*-xylylene-bis(thioacetic) acid in the form of white powder. Mp 149 - 150 ^oC (ref.[17] 149 ^oC).

^1H NMR ($CDCl_3$): 3.15 (4H, s, -SCH_2CO), 3.85 (4H, s, -$ArCH_2S$), 7.38-8.15 (4H, m, ArH,), 10.20 (2H, s, -COOH). Anal. Calc. for $C_{12}H_{14}O_4S_2$ (286.37): C 50.33; H 4.93; S 22.39. Found: C 50.43; H 4.89; S 22.40.

***p*-XBTA** acid synthesized in four steps was obtained as polycrystalline powder. To prepare single crystals suitable for X-ray diffraction, recrystallization of crude *p*-xylylene-bis(thioacetic) acid from a methanol solution was attempted and thus its structure was determined.

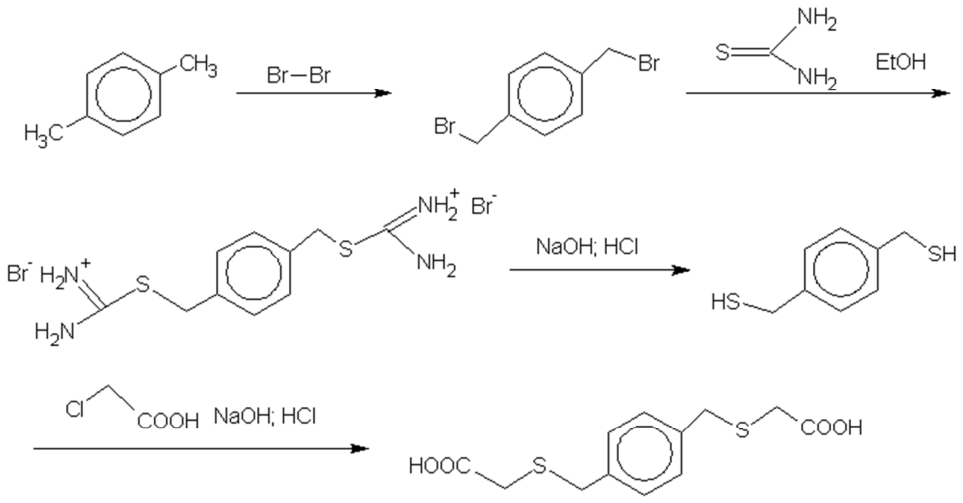

Scheme 2. Schematic representation of four-steps synthesis of *p*-xylylene-bis(thioacetic) acid (*p*-XBTA) (*p*-xylylene was the initial reactant)

Co-crystals synthesis

Co-crystals were prepared by mixing the solutions of 2-amino-4,6-dimethylpyrimidine, with the solution of *p*-xylylene-bis(thioacetic) acid at the molar ratio 2:1, respectively.

(co-1) *p-XBTA (DMP)$_2$* *p-XBTA* (0.040g, 0.14 mmol) was dissolved in DMF (5ml). DMP (0.034g, 0,28 mmol) was dissolved in 5ml DMF. Next, the two solutions were combined and stirred for 5 min. Slow evaporation of the solution at room temperature yielded plate-like single crystals

(co-2) *p-XBTA (DMP)$_2$·2H$_2$O* The ethanol-water (v=20 ml : v=10 ml) mixture was added to *p-XBTA* (0.040g, 0.14 mmol) and the obtained solution was heated at 70˚C and stirred. To DMP (0.034g, 0,28 mmol) there was added the ethanol: water (v=20 ml : v=10 ml) mixture, and the solution was heated at 70˚C while stirring. The two solutions were combined and stirred for 5 min. Colorless needle-like single crystals were obtained after a few days by slow evaporation at room temperature.

p-XBTA (0.040g, 0.14 mmol) and DMP (0.034g, 0,28 mmol) were dissolved in DMSO (4 ml). After a few weeks, needle-like single crystals of **co-2** were harvested.

(co-3) *p-XBTA DMP* Propan-2-ol (15 ml) was added to *p*-XBTA (0.040g, 0.14 mmol) and the obtained solution was heated at 70˚C while stirring. The same solvent (propan-2-ol, (15 ml)) was added to DMP (0.034g, 0.28 mmol) and solution was heated (up to 70˚C) and mixed. The two solutions were combined and stirred for 5 min. Colorless plate-like single crystals were obtained after a few days of slow evaporation at room temperature.

The same procedure was repeated for the synthesis of **co-3** in acetonitrile and ethyl acetate solvents. The amounts of added co-formers and the solvent volumes were the same as for the 2-propanol solution.

Changing the molar ratio of DMP : *p*-XBTA to 3:1 does not affect the final products. Using the same of solvents and their quantity afforded the same three forms of co-crystals as in the case molar ratio 2:1.

ATR-FTIR

Attenuated total reflectance ATR-FTIR spectra were recorded over the range of 4000 - 600 cm^{-1} on the Nicolet 6700 FTIR spectrometer equipped with a universal ATR attachment with a ZnSe crystal.

X-ray analysis

The crystallographic measurements were performed on an Oxford Diffraction Xcalibur CCD diffractometer with the graphite-monochromated Mo K_α radiation (λ = 0.71073 Å). Data sets were collected at 100 K using the ω scan technique, with an angular scan width of 1.0°. The programs CrysAlis CCD and CrysAlis Red[18] were used for data collection, cell refinement, and data reduction. A multi-scan absorption correction was applied. The structures were solved by direct methods using SHELXS-97[19] and refined by the full-matrix least squares on F^2 using SHELXL-97.[19] Calculations were carried out with the WinGX package program.[20] All non-H atoms were refined with anisotropic displacement parameters. All H atoms in ***p*-XBTA** and **co-3** were located from the difference-Fourier maps and refined isotropically. In **co-1** hydrogens attached to aromatic carbon atoms were placed at calculated positions and included in the refinement in the riding model approximation with $U_{iso}(H) = 1.2U_{eq}(C)$. All remaining ones were found in the difference-Fourier maps and refined isotropically. In turn, in **co-2** (C)H atoms were placed at calculated positions and refined using the 'riding model'. Water, hydroxyl and amine H-atoms were found in the difference-Fourier maps and refined with isotropic displacement parameters. The summary of crystal data, experimental details, and refinement results are listed in Table 1. The selected bond distances and angles are presented in Table S1 (Supplementary Materials). The molecular plots were drawn with Mercury.[21] The CIF files for each refinement are available from the Supporting Information or can be retrieved from the Cambridge Crystallographic Data Centre (CCDC) (deposition numbers CCDC 1014647-1014650).

Table 1. Summary of crystallographic data and refinement details for ***p*-XBTA** acid and its co-crystals.

Compound	*p*-XBTA	co-1	co-2	co-3
Chemical formula	$C_{12}H_{14}O_4S_2$	$C_{12}H_{14}O_4S_2{\cdot}2(C_6H_9N_3)$	$C_{12}H_{14}O_4S_2{\cdot}2(C_6H_9N_3){\cdot}2H_2O$	$C_{12}H_{14}O_4S_2{\cdot}C_6H_9N_3$
Formula weight	286.35	532.68	568.71	819.03
Crystal system	monoclinic	monoclinic	monoclinic	orthorhombic
Space group	*C*2/c	$P2_1/c$	$P2_1/c$	*C*mca
a (Å)	9.4633(4)	17.637(2)	20.968(3)	32.932(3)
b (Å)	12.6496(4)	4.8355(5)	4.7107(5)	7.9668(5)
c (Å)	10.8834(4)	15.593(2)	14.401(2)	15.2754(8)
β (°)	104.267(4)	96.07(1)	95.31(1)	90
V (Å^3)	1262.64(8)	1322.3(2)	1416.4(3)	4007.7(5)
Z	4	2	2	8
T (K)	100(2)	100(2)	100(2)	100(2)
Crystal colour and shape	colourless prism	colourless plate	colourless needle	colourless plate
D_{calc} (g cm^{-3})	1.506	1.338	1.333	1.357
μ (mm^{-1})	0.425	0.243	0.237	0.294
Refl. collected	2837	8987	9304	5299
Refl. unique	1452	3027	3235	2326
$R_{(int)}$	0.0204	0.0562	0.0654	0.0337
Refl. with $I>2\sigma(I)$	1358	2354	2308	1617
Refined parameters	110	187	190	174
GooF on F^2	1.153	1.041	1.105	0.902
R_1 ($I>2\sigma(I)$)	0.0320	0.0579	0.0651	0.0351
wR_2 (all data)	0.0841	0.1565	0.1534	0.0758
$\varrho_{res}^{min/max}$ / e·Å^{-3}	-0.20/0.55	-0.29/0.57	-0.31/0.43	-0.19/0.37

Thermal analysis

The thermal behaviour of the compounds was investigated with the aid of a Setsys 16/18 (Setaram) thermal analyzer, registering the TG, DSC and DTG curves. The samples (5 mg)

were heated in a ceramic crucible in the temperature range 30 - 700°C in the flowing air atmosphere (v = 1 dm^3 h^{-1}) with a heating rate of 10°C min^{-1}.

Results and discussion

Analysis of co-crystals 1, 2 and 3 via infrared spectroscopy

Infrared spectroscopy is a reliable technique to ascertain the formation of co-crystals. Usually, formation of co-crystals is reflected in their IR spectra by shifting characteristic stretching vibrations (ν) bands of co-formers. A comparison of the ν_s bands of shifts gave an estimate of the relative strengths of the hydrogen bonds formed between the functional groups.[22] The detailed peaks assignment for the free co-formers and each co-crystal is given in Table S2 (Supplementary Materials). The analysis of the ATR-FTIR spectra of the compounds prepared in this study confirms formation of co-crystals in all cases. In general, contribution of D-H group (where D is an atom being of proton donor) in hydrogen bonds or other weak interactions during co-crystal formation decreases the frequency and intensity of stretching vibrations while bandwidth is increased. These observations have remained true for most of the hydrogen bonded systems.[23-25]

The crystal structures of co-crystals 1, 2 and 3 are stabilized *via* hydrogen bonds where strong hydrogen bonding groups such as COOH, NH_2, H_2O as well as pyridine N-atoms are preferred, so vibrations of these functional groups are associated with the largest shifts in the ATR-FTIR spectra compared to those of co-formers. The co-crystals display the stretching frequency bands for both co-formers with associated shifts confirming the formation of a new phase (Figs 2a, 2b).

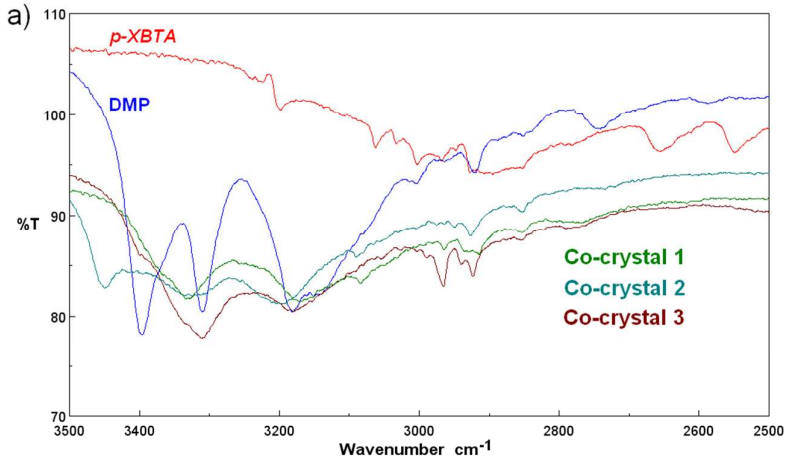

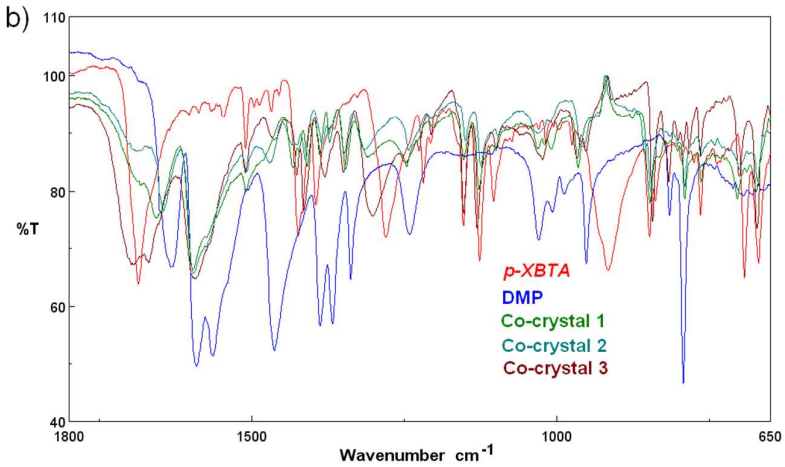

Fig. 2 ATR-FTIR spectra of ***p*-XBTA**, **DMP** and **co-1**, **co-2**, **co-3** in the ranges: a) 3500-2500 cm^{-1} and b) 1800-650 cm^{-1}

The ATR-FTIR spectrum of ***p*-XBTA** shows broad band in the range 3200-2400 cm^{-1} with the strongest submaxima at 2656 and 2549 cm^{-1}. These absorption peaks are derived from stretching vibrations of hydrogen bonded hydroxyl groups ν(OH)[24], from carboxylic groups and the C−H stretching modes ν(C-H) from methylene groups and aromatic ring. Such bands bear out on association of acid molecules in the crystal structure.

As can be seen from Fig. 2a , these bands are not visible in the spectra of co-crystals. Only in **co-2**, there is a band at 3449 cm^{-1} which can be assigned to stretching vibrations ν(OH) of water molecules.[26] The most intense band in the ATR-FTIR spectrum of the acid occurring at 1686 cm^{-1} is associated with the carbonyl stretching vibrations ν(C=O) of COOH groups. This band "almost" disappear in **co-1** and **co-2** while in **co-3**, ν(C=O) band has a medium intensity (Fig. 3). The changes in the intensity of such bands can be explained by participation of C=O groups in hydrogen bonds. The following difference observed among the spectrum of ***p*-XBTA** and its co-crystals is connected with shift of the band at 1280 cm^{-1} related to vibrations of -COOH groups (ν(C-O)+β(OH)) to higher frequencies (1311, 1315 and 1302 cm^{-1} for **co-1**, **co-2** and **co-3**, respectively). Additionally, in the spectrum of free acid, strong band at 916 cm^{-1} can be observed due to out-of-plane deformation vibrations of carboxylic OH group.[26] In the spectra of co-crystals this band disappears.

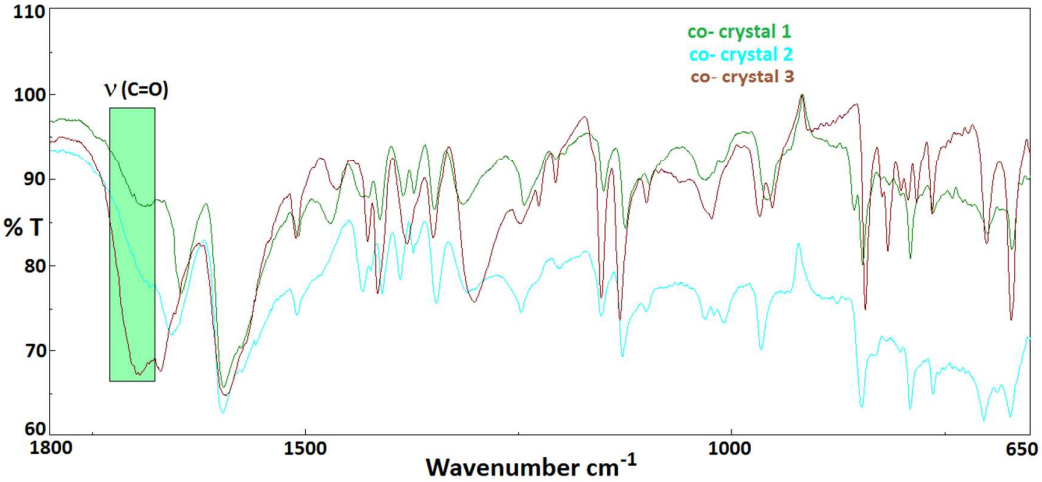

Fig.3 ATR-FTIR spectra of **co-1** and **co-2** (monoclinic form) and **co-3** (orthorhombic form) in the range 1800-650 cm^{-1}

The ATR-FTIR spectrum of free DMP exhibits two bands at 3394 and 3306 cm^{-1} assigned to the asymmetric $\nu_{asym}(NH_2)$ and symmetric $\nu_{sym}(NH_2)$ stretching vibrations of amine group. This group is involved in N-H…N hydrogen bonds with different geometry.[27] In all co-crystals spectra, shifts of these bands to lower frequencies are observed. The greatest shift of $\nu_{asym}(NH_2)$ bands is observed in the case of **co-3** where the strongest N-H···O_{car} hydrogen bonds appear. The infrared stretching vibrations with the associated shifts (in brackets) in comparison with DMP are given in Table 2.

Table 2 Infrared stretching vibrations for amine NH_2 groups in free DMP and co-crystals[a]

Peak assignment	DMP	Co-1	Co-2	Co-3
amine $\nu(NH_2)_{asym}(cm^{-1})$	3394	3332(-62)	3324(-70)	3311(-83)
(D…A distance/ Å)		N-H…$O_{(carb)}$/3.002 N-H…$N_{(pyrim)}$/3.060	N-H…$O_{(carb)}$/2.947 N-H…$O_{(H2O)}$/3.077	N-H…$O_{(carb)}$/2.854
amine $\nu(NH_2)_{sym}(cm^{-1})$	3306	3170(-136)	3192(-114)	3180(-126)

[a]The values given in the brackets are the frequency shifts in comparison with the corresponding groups in the co-former DMP

X-ray crystallography

Molecular and crystal structure of p-XBTA

The title compound crystallizes in the monoclinic *C*2/*c* space group (Table 1) with a half of molecule in the asymmetric unit. The compound is a flexible symmetric dicarboxylic acid which bears two S atoms in the aliphatic side-chains of benzene ring. The centrosymmetric molecule of *p*-XBTA, with the inversion centre at the mid-point of the aromatic ring, is non-planar (Fig. 4a). The thioacetic moieties are strongly twisted away from the plane of xylylene unit due to sp^3 hybridization of sulphur and methylene carbon atoms.

The orientation of the central moiety in relation to the carboxylic group is defined by the C1-C2-S1-C3 torsion angle (Table S1, Supplementary Materials). In ***p*-XBTA** atom C1 adopts a -*synclinal* (-*sc*) orientation with respect to xylylene C3. In turn, the thioacetic S1 atom is -*anticlinal* (-*ac*) with respect to hydroxyl O1 and *anticlinal* (+*ac*) to phenyl C5 atom. The dihedral angle between the best planes of benzene ring and carboxylic group is 58.0(1)°. Due to symmetry, the carboxylic groups adopt *trans*-coplanar configuration with respect to the phenyl unit. Twisting of the carboxylic group from the plane of the central ring is also observed in other phenylacetic acids.[28-30] The bent conformation of the aliphatic side-chains is stabilized *via* intramolecular, three-centre C5-H5…O2, C3-H3a…O2 hydrogen bonding (Table 3, Fig. 4a). The carboxylic groups in ***p*-XBTA** adopt the *syn* conformation and the O1-C1-O2 angle of 123.7(1)° is typical of protonated carboxylic acids.[31] All remaining bond lengths and angles (Table S1, SM) are in accordance with the standard values.[32]

The supramolecular network of ***p*-XBTA** is built up from centrosymmetric hydrogen-bonded dimers with $R_2^2(8)$ ring motif (Fig. 4b). This $R_2^2(8)$ homosynthon is favoured over catemar motif in benzenecarboxylic acids.[31] The acid molecules form infinite 1-D chains extending along the [101] direction, in which the molecules are linked to each other *via* strong, linear hydrogen bonds of O–H···O type (Table 3). Along with strong hydrogen bonds, weak interactions contribute to self-assembly processes in ***p*-XBTA**. These contacts can be observed between one of H-atoms of the methylene group of acetic moiety and O-atom the carboxylic groups as well as between sulphur atom and C_{ar}–H donor of benzene ring. As can be seen from Figs 4b and 4c, the former C2-H2b…O1 (symmetry code: 1/2-*x,* 1/2-*y,* 2-*z*) interactions link adjacent [101] molecular chains into (-111) layers, whereas the latter C5–H5…S1 (1/2-*x,* 1/2+*y,* 3/2-*z*) contacts lead to folded (-202) molecular layers. The combination of the motifs gives a complex 3-D supramolecular architecture (Fig. 4d).

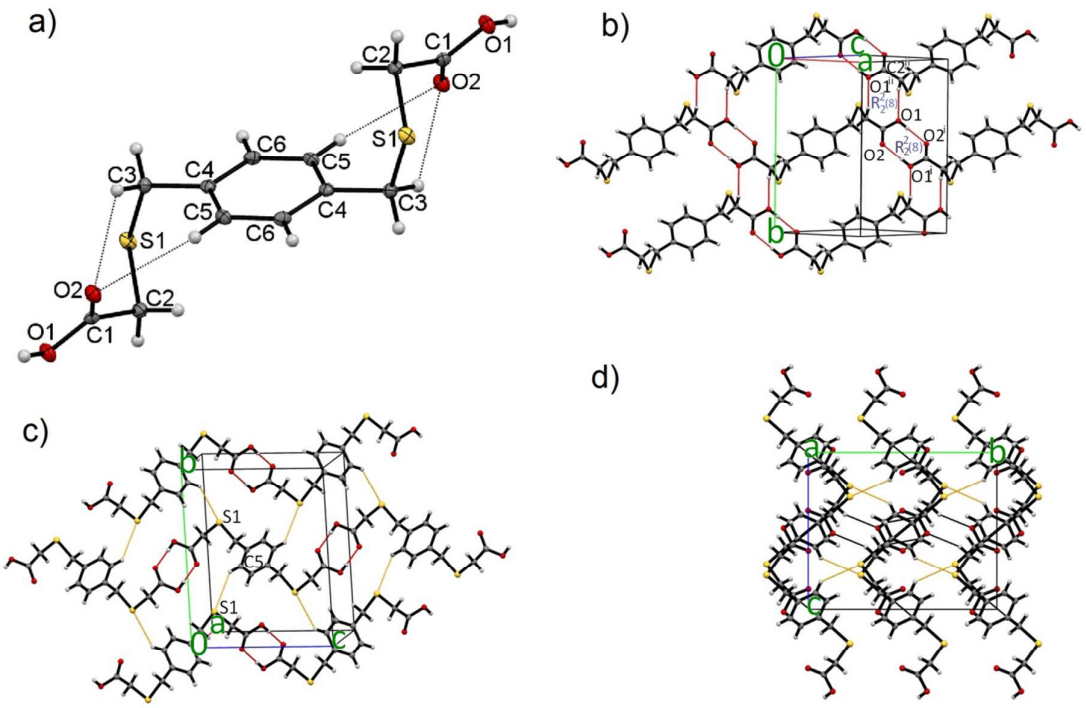

Fig. 4 (a) Molecular structure of ***p*-XBTA** with the atom labelling scheme. (b) (c) Hydrogen-bonded molecular layers, parallel to (-111) and (-202) crystallographic planes, respectively. (d) Crystal packing in view along the *a*-axis. Displacement ellipsoids are drawn at the 50% probability level. Dashed lines indicate hydrogen bonds.

Table 3. Geometries of proposed hydrogen bonds

Bond	D–H /Å	H···A /Å	D–H···A /Å	<D–H···A/°	Symmetry operations
			***p*-XBTA**		
O1–H1o···O2	0.83(2)	1.85(2)	2.677(2)	180(1)	1-*x*, 1-*y*, 2-*z*
C5–H5···O2	0.93	2.64	3.407(2)	140	*x*, *y*, *z*
C3–H3a···O2	0.97	2.59	3.212(2)	122	*x*, *y*, *z*
C2–H2b···O1	0.96	2.62	3.543(2)	162	1/2-*x*, 1/2-*y*, 2-*z*
C5–H5···S1	0.93	2.98	3.903(2)	137	1/2-*x*, 1/2+*y*, 3/2-*z*
			co-1		
O1–H1o···N1	0.90	1.69	2.580(2)	168	*x*, *y*, *z*
N2–H21···O2	0.85	2.17	3.002(2)	169	*x*, *y*, *z*
C5–H5···O1	0.93	2.70	3.365(2)	129	*x*, *y*, *z*
C3–H3a···O1	0.97	2.68	3.284(2)	121	*x*, *y*, *z*
N2–H22···N3	0.80	2.28	3.060(3)	167	-*x*, 2-*y*, 1-*z*
C9–H9···O2	0.93	2.43	3.283(3)	153	*x*, 3/2-*y*, -1/2+*z*
			co-2		
O1–H1o···N1	0.99	1.60	2.583(3)	174	*x*, 1/2-*y*, 1/2+*z*
N2–H21···O2	0.89(3)	2.06(4)	2.947(4)	173(1)	*x*, 1/2-*y*, -1/2+*z*
N2–H22···O1w	0.90(4)	2.20(4)	3.077(4)	165(1)	-*x*, -1/2+*y*, 1/2-*z*
O1w–H1w···N3	0.88(4)	2.02(4)	2.892(3)	168(1)	*x*, *y*, *z*
O1w–H2w···O1w	0.76(3)	2.05(3)	2.776(3)	159(1)	-*x*, 1/2+*y*, 1/2-*z*

C3–H3a···O1	0.97	2.69	3.332(4)	124	*x*, *y*, *z*
C5–H5···S1	0.93	2.96	3.605(3)	127	1-*x*, 1/2+*y*, 3/2-*z*
C9–H9···O2	0.93	2.46	3.349(3)	161	*x*, 1+*y*, *z*
co-3					
O1–H1o···N1	1.02(3)	1.60(3)	2.611(2)	171(1)	*x*, 1/2 -*y*, -1/2+*z*
N2–H21···O2	0.90(2)	1.96(2)	2.854(1)	172(1)	*x*, 1/2-*y*, 1/2+*z*
C10–H10c···O2	0.93(2)	2.61(2)	3.381(2)	141(1)	*x*, *y*, *z*
C3–H3b···S1	0.99(2)	2.97(2)	3.800(2)	142(1)	*x*, 1/2+*y*, 3/2-*z*
C2–H2a···S1	0.95(2)	2.92(2)	3.809(2)	156(1)	*x*, -1/2+*y*, 3/2-*z*

*Crystal structure of p-XBTA (DMP)$_2$ (**co-1**)*

The crystal structure of *p*-XBTA (DMP)$_2$ belongs to the monoclinic $P2_1/c$ space group. The asymmetric unit of **co-1** contains a half of acid molecule and one molecule of 2-amino-4,6-dimethylpyrimidine (Fig. 5a). The bond distances in the carboxylic groups of the acid (C1-O1: 1.310(3) Å; C1-O2: 1.225(3) Å) as well as those in the pyrimidine ring (C7-N1: 1.361(3) Å; C7-N3: 1.359(3) Å) confirm that both co-formers are in their neutral form in the crystal. The overall geometry of the acid in **co-1** is quite similar to that observed in ***p*-XBTA** except for the relative orientation of –COOH group with respect to the central moiety. As indicated from the O1-C1-C2-S1 torsion angle (91.1(2)°) the hydroxyl O1 atom in **co-1** is *+ac* with respect to the S1 atom, *vs* the *-ac* conformation (torsion angle: -97.1(1)°) observed in the crystal of the pure acid. The dihedral angle between the best planes of benzene ring and carboxylic group is 41.2(2)°. Another conformational difference between the molecules results from small rotation around the C3-C4 bond (Table S1, SM). Opposite orientation of the carboxylic group is induced by hydrogen-bonding patterns. Every acid molecule in **co-1** is connected with two DMP molecules through the pairs of hydrogen bonds: O_{car}–H···N_{pyr} and N_{pyr}–H···O_{car} with a graph set of $R_2^2(8)$ (Table 3, Fig. 5a). Additionally, the observed self-association of the base molecules is observed due to preferences of DMP for formation of homosynthon $R_2^2(8)$ via N-H···N hydrogen bonds (Fig. 5b). In the current structure, characteristic discrete motifs composed of a pair DMP molecules and two acid can be distinguished (Fig. 5b). The same association mode was observed in some others, previously reported co-crystals of DMP with different monocarboxylic acids [12, 33-36] as well as with glutaric, adipic[11] or terephthalic acid.[37, 38] The translation related heterotetramers (LHT) form molecular tapes parallel to (212) crystallographic plane. The adjacent tapes are packed to form 2-D layers stabilized via weak C11-H11b···π_{pyr} ($d_{C11\cdots\pi cent}$=3.451(2) Å, $d_{H11b\cdots\pi cent}$=2.60 Å, <C11-H11b···π_{cent}=157°; symmetry code: *x*, *y*+1, *z*) interactions and π-stacking contacts (Fig. 5d) involving almost coplanar pyrimidine rings and carboxylic groups. The other non-covalent forces stabilizing the 3-D network of **co-1** are weak interactions of C_{CH_2}-H···O type (Table 3, Fig. 5c) occurring between the adjacent perpendicular layers.

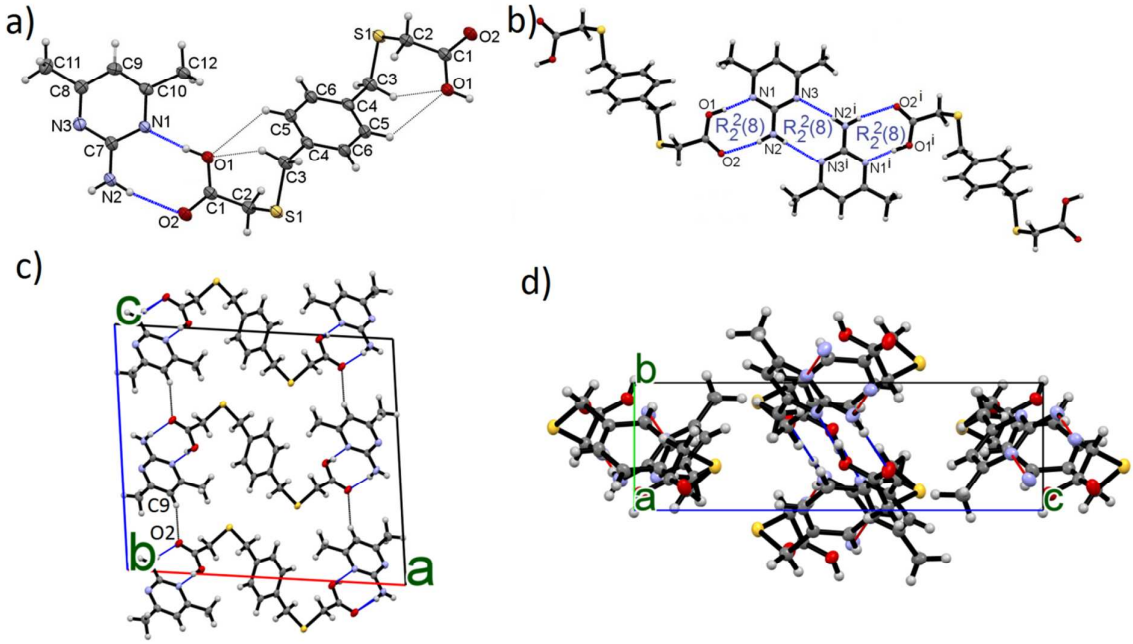

Fig.5 Part of the crystal structure of **co-1** showing: (*a*) molecular structure of co-formers linked via strong O1-H1o…N1 and N2-H21…O2 hydrogen bonds; (*b*) linear heterotetramer (LHT) stabilized by strong hydrogen bonds; (*c*) crystal packing in view along the *b*-axis; (*d*) crystal packing in view along the *a*-axis. Dashed lines indicate hydrogen bonds.

*Co-crystal description of p-XBTA (DMP)$_2$·2H$_2$O (**co-2**)*

p-Xylylene-bis-(thioacetic) acid and 2-amino-4,6-dimethylpyrimidine form a 1:2 co-crystal of the formula *p*-XBTA (DMP)$_2$·2H$_2$O (**co-2**) (Fig. 6a) during crystallization from DMSO or ethanol-water mixture. The hydrate crystallizes in the monoclinic $P2_1/c$ space group, with a half of *p*-XBTA, one DMP and one water molecule in the asymmetric unit. Inclusion of the water molecules into the crystal does not entail any significant changes in the overall geometry of the acid compared to that observed in **co-1**. The only noticeable conformational changes result from small rotation around S1-C2 and C3-C4 bonds (Table S1, SM). Much more visible differences are in supramolecular association modes. The most characteristic motif observed in **co-2** is a trimer composed of two DMPs and one acid molecule through the predominant $R_2^2(8)$ heterosynthons (Fig. 6b). Each acid molecule is connected with two adjacent 2-amino-4,6-dimethylpyrimidine molecules *via* a pair of hydrogen bonds: O_{car}–H···N_{pyr} and N_{pyr}–H···O_{car} creating a $R_2^2(8)$ ring motif (Table 3, Figs 6b,c). It is worth noting that each DMP molecule is engaged only once in formation of the above motif. The other pyrimidine nitrogen atom participates in O_w-H···N_{pyr} hydrogen bonds. Additionally, the amine group is involved in N-H···O_w interactions with another water molecule (Table 3). Water molecules play the crucial role in the architecture of the studied co-crystal. As can be seen from the crystal packing view along the *b*-axis (Fig. 6c), they serve as a 'molecular glue' filling a free space between the adjacent trimeric motifs. Hydrogen-bonded water molecules

are propagated along the *b*-axis forming 1-D helical chains (Fig. 6d) with a distance between the neighbouring oxygen atoms equal to 2.776(3) Å. Chains of water molecules are accommodated between columns of 2-amino-4,6-dimethylpyrimidines. Apart from strong hydrogen bonds the 3-D structure of **co-2** is stabilized by weak intermolecular C_{ar}–H···S and C_{pyr}–H···O_{car} interactions (Table 3, Fig. 6c).

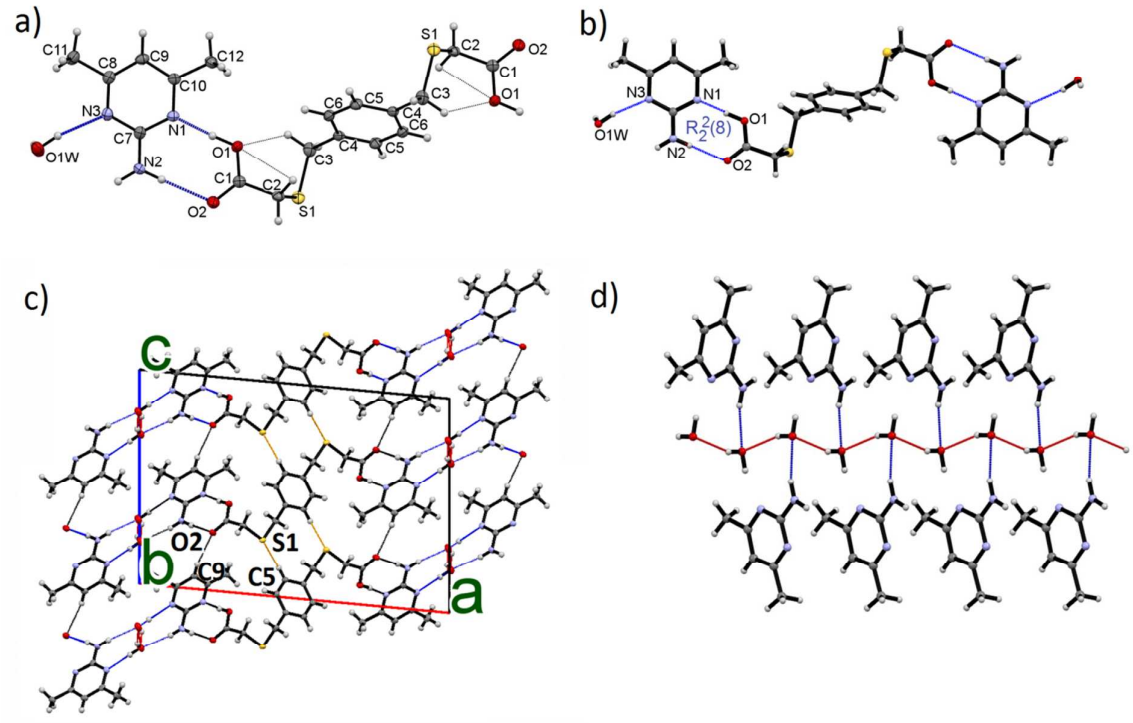

Fig. 6 (a) Molecular structure of co-formers in **co-2** linked via strong hydrogen bonds; (b) hydrogen-bonding patterns; (c) crystal packing in view along the *b*-axis; (d) helical chains of water molecules in view along *a*-axis. Dashed lines indicate hydrogen bonds.

*Crystal structure of p-XBTA DMP (**co-3**)*

The orthorhombic form of *p*-XBTA DMP crystallizes in the *C*mca space group. This co-crystal can be grown from the acetonitryle, ethyl acetate or propan-2-ol solvents. The asymmetric unit of **co-3** comprises a half of the acid and a half of 2-amino-4,6-dimethylpyrimidine molecule (Fig. 7a). Each acid molecule is associated with two base molecules through two pairs of hydrogen bonds: O_{car}–H···N_{pyr} and N_{amine}–H···O_{car} (Table 3, Fig. 7b) which form characteristic heterosynthons $R_2^2(8)$. The same heterotrimeric (HT) motif was found in co-crystals of DMP with cinnamic acid,[39] 3-phenylacrylic acid,[12] 3,5- and 3,4-dimethylbenzoic acids.[36] The trimeric units are repeated along the *a*-axis forming infinite chains. The DMP molecules in such a motif are coplanar. On the contrary, reflected through a mirror plane *p*-XBTA molecules are not coplanar; the best-planes of their phenyl rings form an angle of 19.0(1)°. The crystal packing view along the *a* axis (Fig. 7c) shows that chains are arranged

into the (010) molecular layers stabilized by weak C_{CH_3}–H···O_{car} hydrogen bonds. Interlayer stabilization is provided by cyclic C_{CH_2}–H···S interactions (Table 3, Fig. 7d).

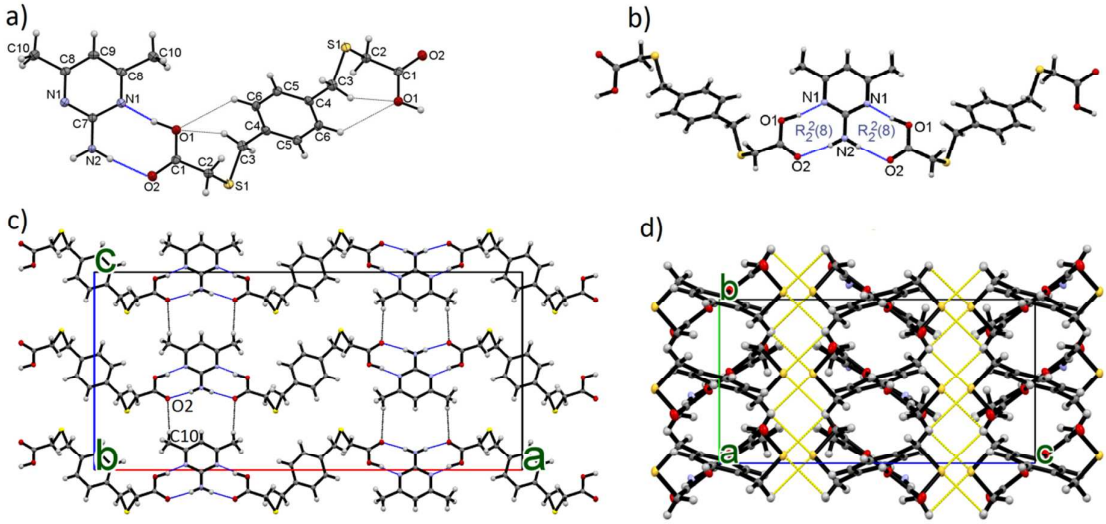

Fig. 7 (a) Molecular structure of co-formers in **co-3** linked via strong O1-H1o…N1 and N2-H2a…O2 hydrogen bonds; *(b)* heterotrimer (HT) stabilized by strong hydrogen bonds; (c) crystal packing in view along the *b*-axis; (d) crystal packing in view along the *a*-axis. Dashed lines indicate hydrogen bonds.

Thermal analysis

Detailed TG/DSC experiments were carried out for each co-crystal to study the thermal behaviour in comparison with that of co-formers. The TG and DSC curves for **DMP**, ***p*-XBTA** and co-crystals are presented in Figures 8 and 9. As can be seen from the TG curves, thermal decomposition of obtained co-crystals is entirely different from that of co-formers. Additionally, diverse chemical composition and crystal structures of co-crystals give rise to different ways of their thermal decomposition. The DSC curves for all compounds showed a single endothermic effect corresponding to the melting points (**DMP**: 153.0°C; ***p*-XBTA**: 153.0°C; **co-1**: 152.5°C; **co-2**: 150.2°C; **co-3**: 156.7°C). The melting point of co-crystals was distinct from either of the individual components confirming the formation of new phases. Very small differences in the melting point values between the co-crystals and co-formers are due to the same melting point ranges of both single components. The presence of water molecules in **co-2** was confirmed by thermal analysis. The **co-2** hydrate, showed two endothermic effects where the first (110°C) is connected with loss of water molecules. The TG curve confirmed the effect of a loss of water (~5.9% of the total weight) that matched approximately to one water molecule in the asymmetric unit (Fig. 9). The analysis of the melting points of all co-crystals reveals that the orthorhombic **co-3** displays an improved thermal stability over the free DMP component, while both monoclinic forms (**co-1** and **co-2**) remain nearly the same showing decreased thermal stability compared to that of DMP.

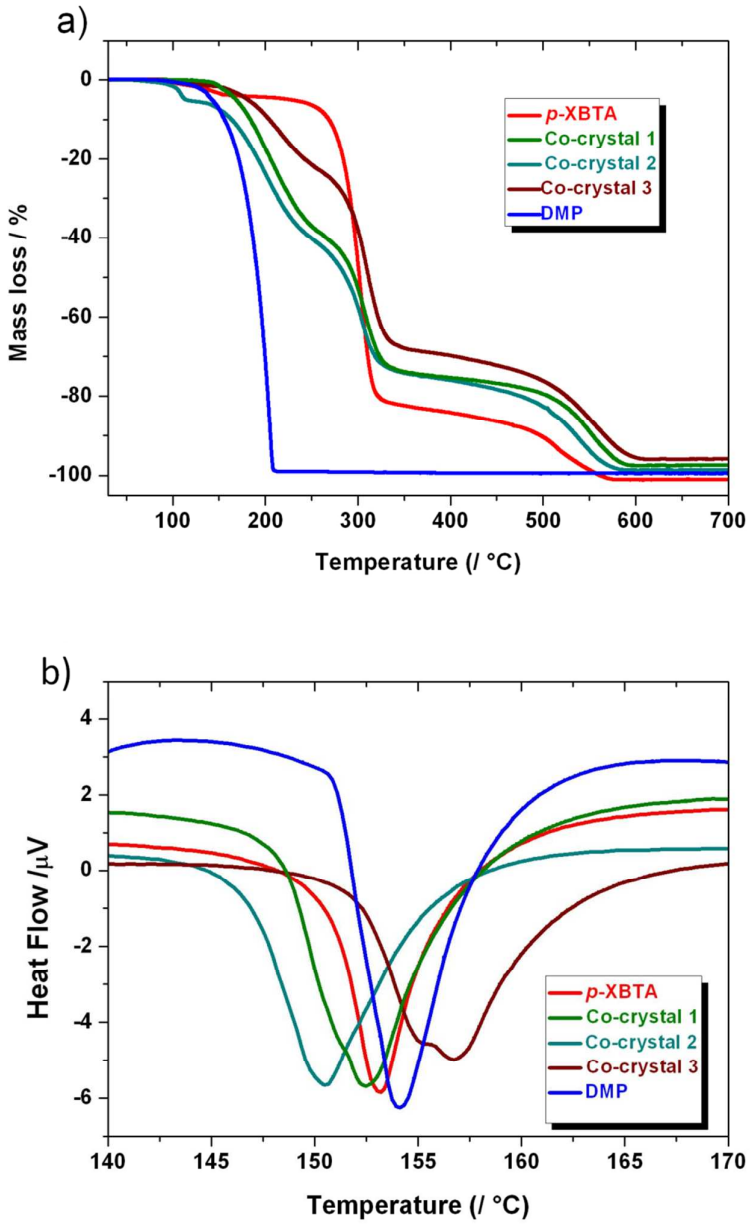

Fig. 8 TG (**a**) and DSC (**b**) curves of ***p*-XBTA**, DMP and **co-1**, **co-2, co-3**

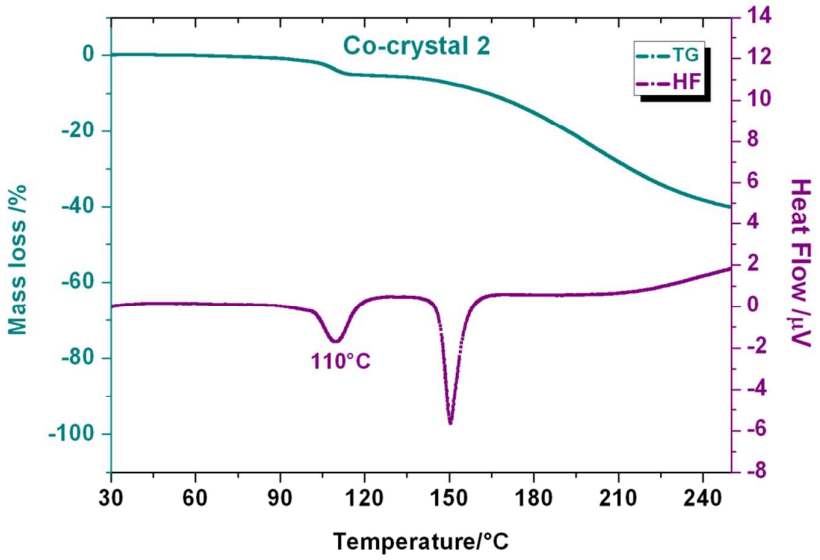

Fig. 9 TG and DSC curves of **co-2**

Conclusions

New flexible thiocarboxylic acid and its co-crystals with DMP were synthesized and characterized thoroughly by single crystal XRD, TG, DSC and ATR-FTIR. Depending on the solvent used for crystallization, three different forms of co-crystals have been isolated. The acid molecules are connected via pairs of O–H···O hydrogen bonds into the 1-D infinite chains which are further associated into the 3-D supramolecular network.

In all three forms of co-crystals acid binds with the DMP via N-H···O and O-H···N hydrogen bonds. In **co-1**, the formation of linear heterotetramer is observed. Notably, **co-2** represents the first example of hydrated form of the co-crystal of 2-amino-4,6-dimethyl pyrimidine with carboxylic acid. In the above-mentioned co-crystal form, pair of water molecules linked trimeric moieties composed of two DMP and one acid molecule. The hydrated form **co-2** was formed from the C_2H_5OH/H_2O mixture or DMSO solvent. Water as a good hydrogen bonds donor competes with p-XBTA acid in interaction with the DMP base forming $O\text{-}H_{(water)}\cdots N$ connection.

The water molecules in hydrated co-crystal play the role of 'molecular glue' filling the free space in the crystal. Formation of hydrated co-crystal from the DMSO solvent can be explained by slow evaporation of this solvent and absorption of the moisture from the air.

The crystal structure of **co-3** consists of heterotrimers. The hydrogen bonding supramolecular synthons observed in the structures are consistent with the fact that the strong acceptors prefer strong donors and the weak acceptors prefer the weak donors.

The analysis of the melting points of all co-crystals reveals that the orthorhombic form of **co-3** displays an improved thermal stability.

In conclusion, this work indicates that p-xylylene-bis(thioacetic) acid is a good participant in hydrogen-bonding networks for the formation of acid-base molecular co-crystals.

References

1. L. R. MacGillivray and J. L. Atwood, *J .Am. Chem. Soc.*, 1997, **119**, 6931-6932.
2. S. J. Dalgarno, J. L. Atwood and C. L. Raston, *Cryst. Growth Des.*, 2006, **6**, 174-180.
3. E. Ishow, C. Bellaiche, L. Bouteiller, K. Nakatani and J. A. Delaire, *J. Am. Chem. Soc* ., 2003, **125**, 15744-15745.
4. N. Lemaitre, A. J. Attias, I. Ledoux and J. Zyss, *Chem. Mater.*, 2001, **13**, 1420-1427.
5. J. S. Huang and M. Kertesz, *J. Am. Chem. Soc.*, 2003, **125**, 13334-13335.
6. B. Moulton and M. J. Zaworotko, *Curr. Opin. Solid St. M.*, 2002, **6**, 117-123.
7. G. J. McManus, J. J. Perry, M. Perry, B. D. Wagner and M. J. Zaworotko, *J .Am. Chem. Soc*, 2007, **129**, 9094-9101.
8. N. Shan and M. J. Zaworotko, *Drug Discov. Today*, 2008, **13**, 440-446.
9. S. Aitipamula, R. Banerjee, A. K. Bansal, K. Biradha, M. L. Cheney, A. R. Choudhury, G. R. Desiraju, A. G. Dikundwar, R. Dubey, N. Duggirala, P. P. Ghogale, S. Ghosh, P. K. Goswami, N. R. Goud, R. R. K. R. Jetti, P. Karpinski, P. Kaushik, D. Kumar, V. Kumar, B. Moulton, A. Mukherjee, G. Mukherjee, A. S. Myerson, V. Puri, A. Ramanan, T. Rajamannar, C. M. Reddy, N. Rodriguez-Hornedo, R. D. Rogers, T. N. G. Row, P. Sanphui, N. Shan, G. Shete, A. Singh, C. C. Sun, J. A. Swift, R. Thaimattam, T. S. Thakur, R. K. Thaper, S. P. Thomas, S. Tothadi, V. R. Vangala, N. Variankaval, P. Vishweshwar, D. R. Weyna and M. J. Zaworotko, *Cryst. Growth Des.*, 2012, **12**, 2147-2152.
10. C. B. Aakeröy, A. B. Grommet and J. Desper, *Pharmaceutics*, 2011, **3**, 601-614.
11. S. Ebenezer and P. T. Muthiah, *Cryst. Growth Des.*, 2012, **12**, 3766-3785.
12. S. Ebenezer, P. T. Muthiah and R. J. Butcher, *Cryst. Growth Des.*, 2011, **11**, 3579-3592.
13. J.Bernstein, R. E. Davis, L. Shimoni,. N.-L. Chang, *Angew. Chem., Int. Ed. Engl.*, 1995, **34**, 1555−1573.
14. F. Allen, *Acta Crystallogr. B*, 2002, **58**, 380-388.
15. X.-Y. Wang, S.-Q. Liu, C.-Y. Zhang, G. Song, F.-Y. Bai, Y.-H. Xing and Z. Shi, *Polyhedron*, 2012, **47**, 151-164.
16. P. Zhang and D. R. Bundle, *Isr. J. Chem.*, 2000, **40**, 189-208.
17. J.-H. Wang, Z. Zhang and Y.-L. Feng, *Synthetic Commun.*, 1993, **23**, 373-377.
18. C*rysAlis PRO*, Agilent Technologies Ltd, Yarnton, Oxfordshire, UK, **2013**
19. G. Sheldrick, *Acta Crystallogr. A*, 2008, **64**, 112-122.
20. L. J. Farrugia, *J. Appl. Crystallogr.*, 1999, **32**, 837-838.
21. C. F. Macrae, P. R. Edgington, P. McCabe, E. Pidcock, G. P. Shields, R. Taylor, M. Towler and J. v. d. Streek, *J. Appl. Crystallogr.*, 2006, **39**, 453-457.
22. S. Ghosh, P. P. Bag and C. M. Reddy, *Cryst. Growth Des.*, 2011, **11**, 3489-3503.
23. E. Arunan, G. R. Desiraju, R. A. Klein, J. Sadlej, S. Scheiner, I. Alkorta, D. C. Clary, R. H. Crabtree, J. J. Dannenberg and P. Hobza, *Pure Appl. Chem.*, 2011, **83**.
24. K. Giese, M. Petković, H. Naundorf and O. Kühn, *Phys. Rep.*, 2006, **430**, 211-276.
25. B. R. Jali and J. B. Baruah, *J. Chem. Crystallogr.*, 2013, **43**, 531-537.
26. R. Silverstein and F. Webster, *Spectrometric identification of organic compounds*, John Wiley & Sons, 2006.
27. W.-W. Fu, Y. Liu, G. Huang and X.-M. Zhu, *Acta Crystallogr. E* , 2012, **69**, o32-o32.
28. J. Sienkiewicz-Gromiuk, H. Głuchowska, B. Tarasiuk, L. Mazur and Z. Rzączyńska, *J.Mol. Struct.e*, 2014, **1070**, 110-116.
29. L. J. Fitzgerald and R. E. Gerkin, *Acta Crystallogr. C*, 1997, **53**, 967-969.
30. B. Sridhar and K. Ravikumar, *Acta Crystallogr. C*, 2007, **63**, o415-o418.
31. L. Leiserowitz, *Acta Crystallogr. B*, 1976, **32**, 775-802.
32. F. H. Allen, O. Kennard, D. G. Watson, L. Brammer, A. G. Orpen and R. Taylor, *J. Chem. Soc. Perkin Trans. 2*, 1987, S1-S19.
33. S. Ebenezer and P. T. Muthiah, *Acta Crystallogr. E*, 2010, **66**, o516.

34. S. Goswami, S. Jana, A. Hazra, H.-K. Fun and S. Chantrapromma, *Supramol. Chem.*, 2008, **20**, 495-500.
35. A.-L. Meng, J.-E. Huang, B. Zheng and Z.-J. Li, *Acta Crystallogr. E*, 2009, **65**, o1595.
36. T. S. Thakur and G. R. Desiraju, *Cryst. Growth Des.*, 2008, **8**, 4031-4044.
37. P. Devi and P. T. Muthiah, *Acta Crystallogr. E*, 2007, **63**, o4822-o4823.
38. S. Goswami, S. Jana, N. K. Das, H.-K. Fun and S. Chantrapromma, *J. Mol. Struct.*, 2008, **876**, 313-321.
39. K. Balasubramani, P. T. Muthiah, R. K. RajaRam and B. Sridhar, *Acta Crystallogr. E*, 2005, **61**, o4203-o4205.

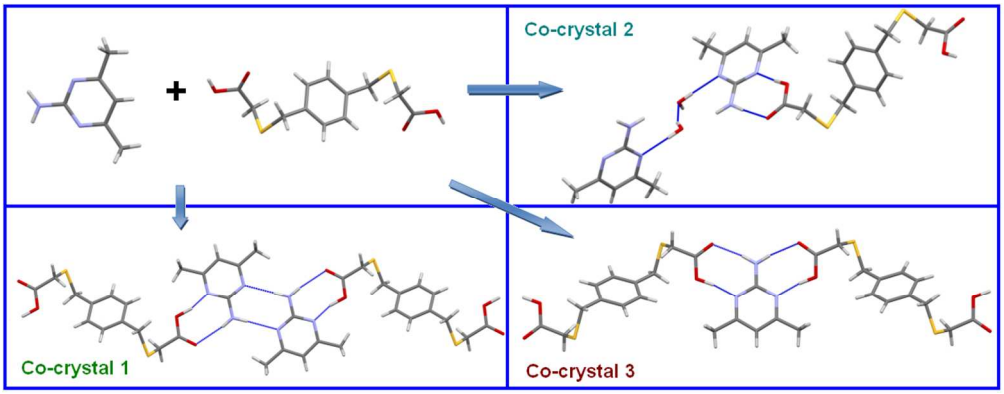

329x128mm (96 x 96 DPI)